A theoretical study of polyelectrolyte effects in protein-DNA interactions: Monte Carlo free energy simulations on the ion atmosphere contribution to the thermodynamics of .lambda. repressor-operator complex formation

B. Jayaram, F. M. DiCapua, and David L. Beveridge

J. Am. Chem. Soc., **1991**, 113 (14), 5211-5215• DOI: 10.1021/ja00014a011 • Publication Date (Web): 01 May 2002

corresponding values approaching the experimental gas-phase ones, whatever the quality of the basis set used in the computation of the wave function. It can also be stated from results for HF and H_2O in Tables IV-VI the well-known tendency of the *split-valence* basis sets to overestimate the magnitude of the dipole moment.[34]

Even though the variation of the dipole moment due to the electron correlation is small, let us emphasize the relevance of the introduction of the electron correlation into the wave function in order to obtain reliable dipole moments at least for some molecules, such as the molecule of CO (see Table VI). Note that, for this molecule, the electron correlation not only reduces the dipole moment considerably, but also changes its sign, which when electron correlation is considered accurately reproduces both the magnitude and the orientation of the experimental gas-phase value.

Finally, results suggest that the dipole moment calculated from the electrostatic charges correctly reflects the magnitude and the orientation of the dipole moment rigorously computed from the wave function, irrespective of the computational level considered. This finding, which points out the higher quality of the electrostatic charges with regard to the Mulliken ones, is especially remarkable in the case of CO. Note that the electron correlation changes the sign of the electrostatic charges of the carbon and oxygen atoms at both CIPSI/G and CIPSI/G+M levels, the corresponding electrostatic dipole moments being very close to the quantum mechanical ones as well as to the experimental value. On the contrary, this change is not observed when dealing with the Mulliken charges.

Conclusion

The preceding discussion points out the reliability of the CIPSI method to quantitatively reproduce the effects of the electron correlation on the electrostatic potential distribution in molecules. Thus, the well depth and location of the MEP minima and the fine essential features of the MEP maps for HF and H_2O, as well as atomic charges and dipoles, determined from CIPSI computations performed by considering the $\{G\} + \{M\}$ space agrees near exactly with those evaluated from full-CI calculations, but at a greatly reduced computational cost. Moreover, the freezing of the inner electrons of non-hydrogen atoms has no significant influence on the modulation of the MEP by the electron correlation.

When MEPs determined at the SCF level are considered, electron correlation generally leads to a small change of the MEP minimum, even though this variation can be nonnegligible for certain molecules, such as CO. In this respect, results demonstrate that the quality of the basis set is of greater importance than the inclusion of the electron correlation. The analysis of MEP maps and profiles indicate that the electron correlation does not have a uniform effect on the electrostatic potential in the whole space surrounding the molecule. Thus, electron correlation has a sizeable influence in those regions near the nuclei, but the MEP computed in regions outside the molecular van der Waals sphere remains largely unaffected by electron correlation. Consequently, the wave function determined at the SCF level is able to reflect with a reasonable accuracy the features of the MEP in the outer regions. It is worth noting that electrostatics dominate the intermolecular interactions in this region.

Acknowledgment. We are indebted to Dr. J. Tomasi and R. Cimiraglia for making available the MEP computer program developed by the Pisa group, which was modified to carry out the present work. We thank the Centre de Càlcul de la Universitat de Barcelona for computational facilities.

Registry No. HF, 7664-39-3; N_2, 7727-37-9; CO, 630-08-0; HCN, 74-90-8; H_2O, 7732-18-5; CH_2O, 50-00-0.

(34) (a) Ditchfield, R.; Hehre, W. J.; Pople, J. A. *J. Chem. Phys.* **1971**, *54*, 724. (b) Binkley, J. S.; Pople, J. A.; Hehre, W. J. *J. Am. Chem. Soc.* **1980**, *102*, 939. (c) Gordon, M. S.; Binkley, J. S.; Pople, J. A.; Pietro, W. J.; Hehre, W. J. *J. Am. Chem. Soc.* **1982**, *104*, 2797.

A Theoretical Study of Polyelectrolyte Effects in Protein-DNA Interactions: Monte Carlo Free Energy Simulations on the Ion Atmosphere Contribution to the Thermodynamics of λ Repressor-Operator Complex Formation

B. Jayaram, F. M. DiCapua, and D. L. Beveridge*

Contribution from the Department of Chemistry, Hall-Atwater Laboratories, Wesleyan University, Middletown, Connecticut 06457. *Received October 1, 1990*

Abstract: We report herein a theoretical calculation of the ion atmosphere contribution to the free energy of association for a protein-DNA complex based on Monte Carlo computer simulations and thermodynamic perturbation theory. The system considered is the dimer of the amino-terminal fragment of the λcI repressor in a complex with a 17 base pair oligonucleotide of DNA, based on the crystal structure of Pabo and Sauer. Only the movements of the small ions (sodium and chloride ions) are considered explicitly, with solvent water modeled as a dielectric continuum (a "primitive model"). The free energies are determined as a function of both distance of separation between the protein and the DNA, each of which is fixed in its respective crystal geometry, and ionic strength at a temperature of 298 K. Results of our simulations indicate that the ion atmosphere contribution to the free energy of association is favorable only at short distances of separation and is at a maximum when the protein approaches the DNA from a distance of ~7 Å. This distance corresponds to the radius of the shroud of condensed counterions around B-DNA. At larger distances of separation between the protein and the DNA, the uncondensed diffuse ionic cloud opposes complexation. The effect known as "counterion release" in the context of DNA-ligand association appears to be short-ranged and a property of the condensed counterions only.

Introduction

The nature of protein-DNA interactions is currently a subject of considerable research interest in molecular biophysics.[1-5] Crystal structures of the protein-nucleic acid complexes reported in the recent literature[6-12] and the concurrent 2D NMR studies[13,14]

(1) Pabo, C. O.; Sauer, R. T. *Annu. Rev. Biochem.* **1984**, *53*, 293-321.
(2) Matthews, B. W. *Nature* **1988**, *335*, 294-295.
(3) Travers, A. A. *Annu. Rev. Biochem.* **1989**, *58*, 427-452.

0002-7863/91/1513-5211$02.50/0

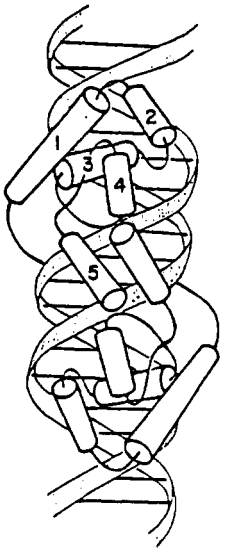

Figure 1. Schematic view of the λ repressor–operator complex (after C. O. Pabo and R. T. Sauer, ref 1).

have significantly enhanced our perspectives on the molecular basis of association. In addition to these structural studies and others now in progress, a parallel understanding of the functional energetics involved appears to be vital to develop a complete picture of the specificity of protein interactions with target sequences on DNA, as well as nonspecific associations.

The essential contributions to the free energy of the association of proteins with DNA come from (a) direct interactions between the protein and the DNA, (b) release of some of the water molecules bound to both protein and DNA, and (c) release of counterions of DNA upon ligand binding (the polyelectrolyte effect).[15-18] The relative magnitudes and importance of each of the possible components to the thermodynamics of protein–DNA association are not at present accurately known. Computer simulations on molecular thermodynamic aspects of the problem can supply a theoretical complement to our growing empirical knowledge on the nature of protein–DNA interactions, provide estimates of the magnitudes of the interactions, and be useful in developing detailed models of the molecular events.

In this study, we investigate the role of polyelectrolyte effects in protein–DNA association via theoretical calculations of free energy based on Monte Carlo simulations. The calculations are carried out on the interaction of λ repressor fragment with a 17 base pair oligonucleotide sequence, taking as a point of departure the crystal structure of Jordan and Pabo.[10] The λ repressor fragment binds to DNA via the "helix–turn–helix" motif as shown schematically in Figure 1.

Background

DNA is a polyanion, and electrostatic stability is achieved by the condensation of counterions. Such a molecular picture has been successful in explaining diverse experimental properties of DNA.[15] Release of condensed counterions is considered to provide an entropic driving force for DNA–ligand complex formation.

A theoretical framework for understanding the role of ion atmosphere in DNA–ligand association has been developed by Manning[15] and Record, Anderson, and co-workers.[16] This theory deals primarily with salt effects on experimentally observed association constants. A plot of log K_{obs} versus log [MX], where K_{obs} is the observed association constant for the DNA–ligand complex and [MX] is the salt concentration, gives a straight line with a slope of $-Z\Psi$. Here Z is the thermodynamic equivalent of the number of counterions released during the DNA–ligand complex formation, and Ψ is assigned a value of 0.88 (which is a sum of 0.76 to account for the condensed counterions and 0.12 to approximate the screening effects due to the remaining uncondensed Debye–Huckel-type ionic cloud in the system).

An analysis of experimental data along the above lines currently forms the primary scheme for studying salt effects and in quantifying the contribution of electrostatics in DNA–ligand binding. A small value for Z or a positive slope is taken to mean that electrostatics is not the driving force, while a large negative slope is taken to imply that electrostatics is the dominant mechanism. The value of Z in such log–log plot is commonly interpreted as indicating the number of ionic interactions in the complex, but this can be disputed. An analysis of the macroscopic data, however simple, elegant, and useful, is not meant to give a detailed account of the molecular mechanism of DNA–ligand complexation.

Theoretical methods based on molecular simulation can describe the complex in terms of intermolecular interactions and provide a basis for developing more detailed molecular models of the process together with estimates of the corresponding energetics. In particular, these methods have been used to treat the free energy of numerous chemical and simple biomolecular processes. The calculations are of course limited due to approximations introduced in configuring the system, in describing the intermolecular interactions, and especially in treating the water. A detailed perspective on free energy simulations applied to biomolecular systems is available in a recent review article from this laboratory.[19]

We report herein Monte Carlo simulations on the interaction of λcI repressor fragment with a 17 base pair oligonucleotide of DNA and obtain estimates of the free energy by using thermodynamic perturbation theory. The protein, DNA fragment, and small ions (counterions and co-ions) are considered explicitly, with solvent water treated as a dielectric continuum (a "primitive model"). Only the small (mobile) ions have motional degrees of freedom in the simulation. The calculations are initially performed at zero added salt (simple electroneutrality) and then extended to include salt effects. A theoretical estimate of the parameter Z for the process is obtained and compared with corresponding experimental values.

Calculations

Free energy simulations via perturbation method[19] are performed on λ repressor–operator complex,[10] at varying distances of separation between the protein and the DNA. The calculations are based on (T,V,N) ensemble Metropolis Monte Carlo simulations[20] at a temperature of 298 K and at added sodium chloride salt concentrations of 0, 25, 50, and 100 mM.

The Cartesian coordinates of the complex were taken from the Brookhaven Data Bank[21] as deposited by Jordan and Pabo.[10] The com-

(4) Steitz, T. A. *Q. Rev. Biophys.* **1990**, *23*, 205–280.
(5) Harrison, S. C.; Aggarwal, A. K. *Annu. Rev. Biochem.* **1990**, *59*, 933–969.
(6) McClarin, J. A.; Frederick, C. A.; Wang, B. C.; Greene, P.; Boyer, H. W.; Grabel, J.; Rosenberg, J. M. *Science* **1986**, *234*, 1526–1540.
(7) Anderson, J. E.; Ptashne, M.; Harrison, S. C. *Nature* **1987**, *326*, 846–852.
(8) Aggarwal, A. K.; Rodgers, D. W.; Drottar, M.; Ptashne, M.; Harrison, S. C. *Science* **1988**, *242*, 899.
(9) Wolberger, C.; Dong, Y.; Ptashne, M.; Harrison, S. C. *Nature* **1988**, *335*, 789–795.
(10) Jordan, S. R.; Pabo, C. O. *Science* **1988**, *242*, 893–899.
(11) Otwinowsky, Z.; Schevitz, R. W.; Zhang, R. G.; Lawson, C. L.; Joachimiak, A.; Marmorstein, R. Q.; Luisi, B. F.; Sigler, P. B. *Nature* **1988**, *335*, 321–329.
(12) Rould, M. A.; Perona, J. J.; Soll, D.; Steitz, T. A. *Science* **1989**, *246*, 1135–1142.
(13) Kaptein, R.; Zuiderweg, E. R. P.; Scheek, R. M.; Boelens, R.; van Gunsteren, W. F. *J. Mol. Biol.* **1985**, *182*, 179–182.
(14) Boelens, R.; Scheek, R. M.; Boom, J. H. v.; Kaptein, R. *J. Mol. Biol.* **1987**, *193*, 213–216.
(15) Manning, G. S. *Q. Rev. Biophys.* **1978**, *11*, 179–246.
(16) Record, M. T., Jr.; Anderson, C. F.; Lohman, T. *Q. Rev. Biophys.* **1978**, *11*, 103–178.
(17) Lohman, T. M. *CRC Crit. Rev. Biochem.* **1986**, *19*, 191–245.
(18) Record, M. T., Jr.; Anderson, C. F.; Mills, P.; Mossing, M.; Roe, J. *Adv. Biophys.* **1985**, *20*, 109–135.
(19) Beveridge, D. L.; DiCapua, F. M. In *Computation of Free Energy for Molecular Systems*; van Gunsteren, W. F., Weiner, P., Eds.; Escom Science Publishers: Leiden, 1989.
(20) Metropolis, N.; Rosenbluth, A. W.; Rosenbluth, M. N.; Teller, A. H.; Teller, E. *J. Chem. Phys.* **1953**, *21*, 1087–1092.

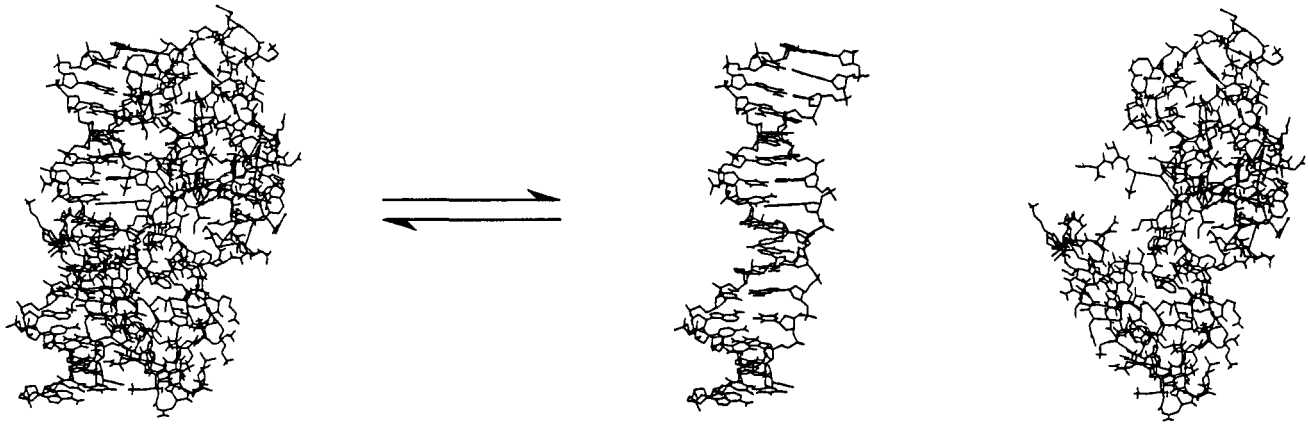

A B

Figure 2. (A) Crystal structure[10] of the λ repressor protein and operator (DNA) in the complexed form. (B) The protein and the DNA shown in (A) are separated by 50 Å. This is accomplished in several small steps. At each step, the whole system is enclosed in a cylindrical box containing sodium counterions and added sodium chloride salt at a temperature of 298 K, and a free energy simulation via perturbation method is performed both in forward and backward directions to determine the ion atmosphere contribution to dissociation/association process. This entire process is then repeated at a different added salt concentration.

plex for our study consists of 17 base pairs of DNA duplex of sequence d(TATCACCGCCAGTGGTA) and 32 phosphates. The λcI repressor fragment considered is a dimer comprising 184 amino acid residues. This complex is enclosed in a cylindrical cell of radius 100 Å, with the cylindrical axis of the box roughly aligned with the helical axis of the DNA. At zero added salt, 32 counterions (sodium ions) are initially added to the system at random locations in the cell, avoiding Van der Waal clashes with the complex. This generates the starting configuration. At finite added salt concentrations, both sodium and chloride ions are added to this system in a similar manner, the number of the small ions added being decided by the concentration of the added salt.

The configurational energy of the system in these simulations involves only intermolecular interactions. Intramolecular interactions within the protein-DNA complex are not considered here. Specifically, the small ions (counterions and co-ions) in the system interact with each other and with the protein-DNA complex. The focus of this study is thus restricted to the ion atmosphere contribution to free energy changes. A (12,1) atom site pairwise interaction energy function, expressed as

$$V_{kl}(r) = (C_{12}/r_{kl}^{12}) + (q_k q_l)/\{\epsilon(r_{kl}) \cdot r_{kl}\} \quad (1)$$

for any two species k and l with charges q_k and q_l and separated by a distance r_{kl}, is used to evaluate the N-particle configurational energy of the system. We assume pairwise additivity in intermolecular interactions. The C_{12} parameters for each atom/ion in the system are adapted from the GROMOS force field.[22] The r^{-12} part of the potential function describes the repulsive interactions and the detailed shape of the complex. Each phosphate on the DNA and each glutamate and aspartate on the protein is assigned a charge of −1. Each arginine and lysine on the protein is assigned a value of +1 consistent with their prototropic form at physiological pH. The net charge on each protein monomer is +1. Both sodium and chloride ions carried a charge of +1 and −1, respectively. The electrostatic interactions are modulated by a dielectric screening function $\epsilon(r)$ including saturation effects as utilized and characterized in an earlier study.[23] Dielectric saturation in the DNA–small ion interactions was found earlier to give a structural description of the ion atmosphere around DNA that is reasonably consistent with the counterion condensation theory and ^{23}Na NMR inferences. Recently, Fenley, Manning, and Olson[24] have used this approach to screening in a new, expanded numerical treatment of counterion condensation theory.

Periodic boundary conditions are imposed on the system in the axial direction and mass conserving diffusive boundary conditions in the radial direction. In addition, one image of DNA is included explicitly in either direction of the cylindrical axis in calculating the configurational energies to account for the polyelectrolyte nature of the DNA. Multiparticle moves (about 2 particles/Monte Carlo step) with a step size of ~1.5 Å were employed to maintain the acceptance ratio at about 50%. Full details of the Monte Carlo methodology as implemented here have been given previously.[23]

The distance of separation between the protein and the DNA in the crystal structure of the complex is assigned the reference value of zero. A series of grid points are established in which the protein is then progressively separated from the DNA radially from an initial distance of 0 Å to a final distance of separation of 50 Å, at a given ionic strength (see Figure 2). The direction of separation is chosen to be the direction in which the spatial extent of the protein is the largest from the helical axis of the DNA. At each step of this separation, a Monte Carlo simulation and free energy determination are performed in both the backward and forward directions. These calculations are then repeated at a series of different ionic strengths.

The perturbation free energy methodology (ref 19 and references therein) is implemented here as follows. Let i represent the reference state and j the perturbed state, and let E_i and E_j be the interaction energies of the complex with the small ions in the two states. Then the ion atmosphere contribution to the free energy difference in going from state i to state j is calculated as

$$A_j - A_i = \Delta A_{ij} = -kT \ln [\langle e^{-(E_j - E_i)/kT} \rangle_i] \quad (2)$$

where angular brackets $\langle\rangle_i$ denote ensemble averages taken with i as the reference state. Both k and T have the usual significance of the Boltzmann constant and temperature. The free energy change for the reverse process of going from state j to i, ΔA_{ji}, can also be calculated from the above expression by interchanging the indices and performing the ensemble averages with j as the reference state. The determinations of ΔA_{ij} and ΔA_{ji} at every step of separation are the forward and backward calculations referred to above. These are carried out here as an additional check of the convergence of the results.

The overall study involved a total of 66 separate simulations. The run length of each simulation is about 100 000 passes, which corresponds to 3.2 million single particle moves at zero added salt and about 24.6 million single particle moves at 100 mM added salt concentration. The free energies as monitored by block averages were seen to converge satisfactorily. (The run lengths appeared to be at least 10 times longer than required as inferred from the cumulative free energy changes for each run.) The first 25 000 passes of each run are treated as equilibration and discarded. Ensemble averages were formed over the last 75 000 passes. The results of these studies are described in the following section.

Results

The theoretically determined free energy change as a function of distance between the protein and the DNA at zero added salt is presented in Figure 3. The free energy at any distance R on the curve is the ion atmosphere contribution to the Helmholtz free

(21) Bernstein, F. C.; Koetzel, T. G.; Williams, G. J. B.; Meyer, E. F., Jr.; Brice, M. D.; Rogers, J. R.; Kennard, O.; Shimanouchi, T.; Tasumi, M. *J. Mol. Biol.* **1977**, *112*, 535.

(22) van Gunsteren, W. F.; Berendsen, H. J. C. *GROMOS86: Groningen Molecular Simulation System*; University of Groningen: Groningen, The Netherlands, 1986.

(23) Jayaram, B.; Swaminathan, S.; Beveridge, D. L.; Sharp, K.; Honig, B. *J. Phys. Chem.* **1990**, *23*, 3156–3165.

(24) Fenley, M. O.; Manning, G. S.; Olson, W. K. *Biopolymers* **1991**, in press.

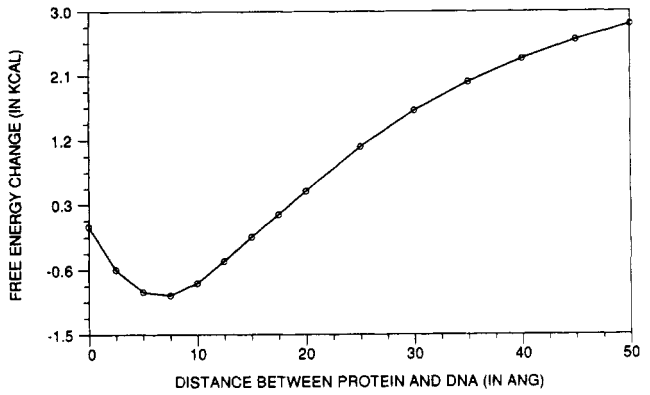

Figure 3. Calculated ion atmosphere contribution to the change in free energy (kcal), shown as a function of distance (Å), for the protein–DNA interaction. The free energy at any distance R on the curve is the ion atmosphere contribution to the Helmholtz free energy of bringing the protein from a distance R to its final complexed state with DNA (R = 0).

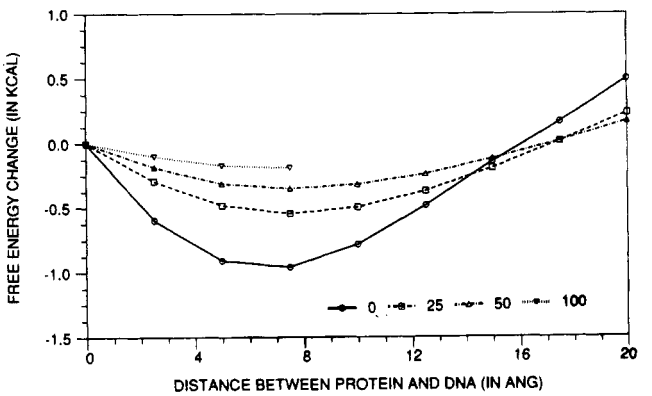

Figure 4. Calculated ion atmosphere contribution to the change in free energy (kcal) shown as a function of distance (Å) between protein and DNA and added sodium chloride salt concentration: solid line with circles, zero added salt; dashed line with squares, 25 mM NaCl; dashed–dotted line with triangles, 50 mM NaCl; and dotted line with inverted triangles, 100 mM NaCl. The free energies at any point on the curves shown have the same connotation as in Figure 3.

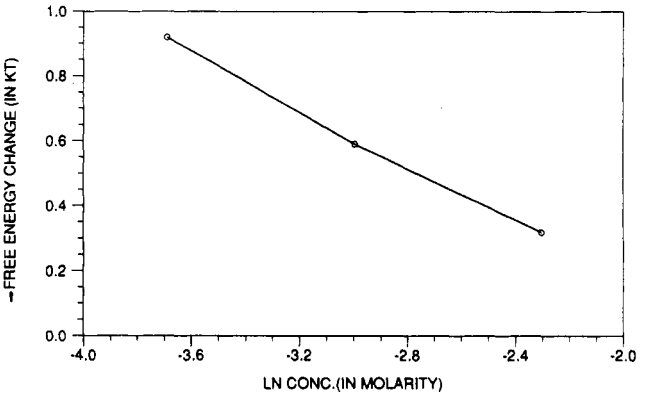

Figure 5. Negative of free energy change in units of kT ($-\Delta A_{min}/kT$), the equivalent of ion atmosphere contribution to ln K_{obs}, shown as a function of ln [NaCl].

energy of bringing the protein from R to its final complexed state (R = 0) with the DNA. This is effectively the ion atmosphere contribution to the potential of mean force for the protein–DNA interaction. We choose R = 0 as the reference state since the usual reference state at $r = \infty$ does not have zero ion atmosphere energy.

Below ~16 Å, the ion atmosphere contribution to the free energy change is negative, favoring association. The enthalpic contribution to the displacement of counterions is endothermic and thus makes a positive contribution to the free energy. Thus, the resulting negative free energy must be a consequence of entropic effects originating in counterion release, and the essential results of the calculation follow conventional wisdom.

The free energy function passes through a minimum at ca. 7 Å from the DNA, which in reference to preceding calculations is essentially the radius ascribed to that part of the ion atmosphere corresponding to condensed counterions. Thus, the calculated free energy due to counterion release is seen to be the largest (ca. −1 kcal/mol) from the point at which the protein first impinges on the condensed counterions. Inside of ~7 Å, the free energy of association is less negative, since only a fraction of the intervening condensed counterions need be released. Since the calculated free energy increases beyond 7 Å, the negative free energy associated with the entropy of counterion release is indicated to be essentially a property of the condensed counterions, the contribution introduced by the uncondensed counterions opposing this in the free energy due to what must be enthalpic effects.

The free energy turns positive at ~16 Å, indicating that the ion atmosphere opposes association at long range. Thus, as a major finding, the calculations indicate that the effect known as "counterion release" in the context of DNA–ligand association is in fact short ranged and a property of the condensed counterions only.

Salt dependence of the free energy profiles are shown in Figure 4 as a function of distance and ionic strength. The minimum in free energy change observed around ~7 Å is seen to become less negative as the salt concentration is increased. This means that the ion atmosphere contribution to the free energy changes diminishes as the salt concentration and thus electrostatic screening is increased. Both distance and ionic strength dependences of the calculated free energies show subtle effects on protein–DNA association.

The calculated free energies as a function of concentration can be used to make a log–log plot analysis of the results analogous to that done for experimental data. We take ΔA_{min} to denote the minimum in $\Delta A(R)$ and the maximum in the contribution of the polyelectrolyte effects. The ΔA_{min} observed in Figure 4 around 7 Å at different concentrations can be plotted as $\{(-\Delta A_{min}/kT) \simeq \ln K_{obs}$ (ion atmosphere)$\}$ versus ln C as shown in Figure 5. The slope of the best fitted straight line passing through the three points shown in Figure 4 is −0.433, which translates into a calculated value of ~0.5 for Z, not in perfect accord with experiment ($Z \approx 2$–3 [10]) but reasonable in view of the approximations.

Discussion

The free energy simulation studies described here suggest that the polyelectrolyte effect, in the region that favors protein–DNA association is on the order of −1 kcal and appears to be short ranged. The ion atmosphere contribution to the free energy of association is favorable and is at its maximum when the protein approaches the DNA from a distance of separation of ~7 Å (Figure 3). This distance corresponds closely to the radius of the counterion condensate around DNA as emerging from counterion condensation theory[15] and independently from our previous Monte Carlo simulations with the dielectric saturation model.[23] This is also the distance adopted in other simulation studies as well[25] to study condensed fraction of counterions around DNA. It is therefore interesting that this distance has come out of the free energy simulations quite naturally.

To facilitate a discussion of the distance dependence of the ion atmosphere contribution to free energies, we have taken a portion of Figure 3 and presented the results with 7.5-Å separation as the reference state in Figure 6. This is essentially a plot of $\Delta A(R_{min}) - \Delta A(R)$, another way of looking at the potential of mean force for the association process. This figure clearly illustrates the contrasting roles of the condensed counterions for distances ≤7 Å, favoring complex formation, and the uncondensed diffuse ion cloud beyond ~7 Å, which favors dissociation.

The short-range behavior of the free energies, that ion atmosphere favors DNA–ligand complexation, is expected on the basis of previous experimental and theoretical studies on similar systems.

(25) Mills, P.; Anderson, C. F.; Record, M. T., Jr. *J. Phys. Chem.* **1985**, *89*, 3984–3994.

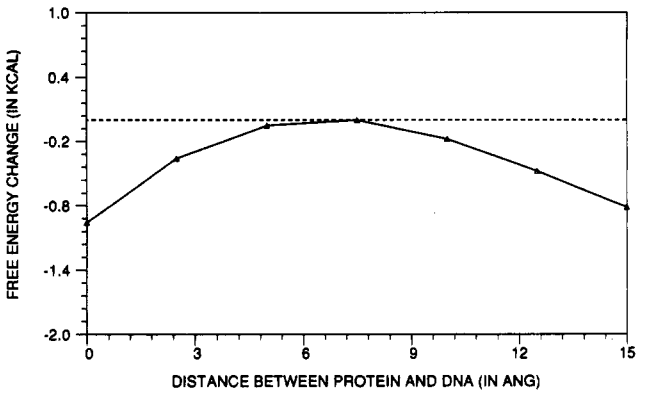

Figure 6. Calculated ion atmosphere contribution to the change in free energy (kcal) shown as a function of distance (Å) between protein and DNA at zero added salt. In the reference state for this figure, protein and DNA are separated by 7.5 Å. The left portion of the free energy curve ($\lesssim\sim$7 Å) shows the influence of the condensed counterions and the right portion ($\gtrsim\sim$7 Å) that of the uncondensed diffuse ionic cloud.

But the long-range (beyond 7 Å) behavior of the free energies, i.e., ion atmosphere opposing complexation, is unanticipated and surprising. A plausible explanation for this observation is that while it costs enthalpically to displace the uncondensed diffuse counterion cloud, there is little entropy gain in the process.

We have performed some additional calculations to see whether this long-range behavior of the free energies is not a result of the particular electrostatic model in use. Some of the simulations were repeated with a simple Coulombic model with the dielectric constant $\epsilon = 80$, instead of a saturation function $\epsilon(r)$. This modification resulted in a similar behavior in $\Delta A(R)$. The magnitudes, however, were slightly smaller as expected since the interaction strength is weaker with a Coulombic model than with a saturation function. Another issue of relevance pertains to the direction of separation. It is probably more justifiable to bring the protein toward DNA from different directions and take an orientational average of the free energies. We carried out simulations by bringing the protein in a radial direction orthogonal to the one presented above and found little difference in the long-range behavior seen above. In short, at this stage, the observation that ion atmosphere disfavors complexation when the distance of separation between the protein and the DNA is large does not appear to be dependent upon the model employed or the radial direction of approach.

A factor that compounds a simple interpretation of the calculated free energies in terms of enthalpies and entropies is the precise role of the charged groups on the protein and their influence on the ion atmosphere. It is likely that the orientation of the charged groups with respect to the DNA helps to magnify the role of ion atmosphere, but no confirmation of this proposal exists. A quantitative split of the total free energies into enthalpic and entropic contributions from each individual constituent of the complex would require several orders of magnitude more machine time and is not currently feasible.

A theoretical determination of Z (Figure 5) via free energy simulations at different salt concentrations gave a value of 0.5 for this system of λ repressor–operator. This is very small compared to the lac repressor–operator system where the corresponding reported value is about 11 ± 2.[18] Jordan and Pabo[10] and references cited therein reported a value of 2–3 for Z in the λ repressor–operator system. They further observed that although the protein contacts at least 10 phosphates on the DNA in the crystal structure of the complex and about the same number of phosphates were seen to be protected in the ethylation interference experiments and hydroxyl radical footprinting studies, the small Z values for this system are consistent with the small number of charged residues that interact with the phosphates.

It is important to note once again that the results presented here are not the total free energy changes for the process. The total would include various contributions such as direct interactions between the protein and the DNA, conformational free energies of the protein and the DNA, and contributions from solvent, in addition to those of ion atmosphere, the only component considered here.

Conclusions

Ion atmosphere appears to favor protein–DNA association when their distance of separation is small. The entropic driving force is at a maximum when the protein approaches the DNA from a distance of $\sim$7 Å. Displacement of the condensed counterions contributes favorably to free energy of DNA–ligand complexation. The exact magnitude of this change probably depends on the nature of the ligand as well as the manner in which electrostatic interactions are treated and the direction of approach of the ligand toward the DNA. For the case of λ repressor–operator considered in this study, it is about −1 kcal at zero added salt. At larger distances of separation between the DNA and the ligand, the uncondensed diffuse ionic cloud opposes complexation. The free energy profiles in general show a complex distance and ionic strength dependence belying the simple expectations from and the assumptions implicit in a log–log plot analysis. The results of this study advocate an element of caution in drawing molecular inferences from an experimental log K versus log C analysis, since opposing effects may underlie the process.

Acknowledgment. This research is supported by grants from NIH (GM-37909) and via the Bristol Myers Corp. and State of Connecticut High Technology Research and Development Award. Supercomputer time was provided on the Cray Y-MP by the Pittsburgh Supercomputing Center.